Supporting Information

Highly Stable Drone-shaped Lanthanide Clusters: Structure, Assembly Mechanism and Crystalline-Amorphous Transitions

Yun-Lan Li,[+] Wen-Wen Qin,[+] Hai-Ling Wang, Zhong-Hong Zhu*, Fu-Pei Liang, and Hua-Hong Zou*

School of Chemistry and Pharmaceutical Sciences, State Key Laboratory for Chemistry and Molecular Engineering of Medicinal Resources, Guangxi Normal University, Guilin 541004, P. R. China *E-mail (Corresponding author): 18317725515@163.com (Z.-H. Zhu), gxnuchem@foxmail.com (H.-H. Zou).

Keywords: High-nuclear lanthanide clusters; Assembly mechanism; Crystalline-amorphous transitions; Magnetic properties

Table of Contents:

Experimental Section

Materials and Measurements.

All reagents were obtained from commercial sources and used without further purification. Elemental analyses for C, and H were performed on a varia MICRO cube. The infrared spectra were carried out on a Pekin-Elmer Two spectrophotometer with pressed KBr pellets. The X-ray powder diffraction (XRD) spectra were measured on a Rigaku D/Max-3c diffractometer with Mo Kα radiation (λ = 0.71073 Å). Thermogravimetric analyses were performed on a PerkinElmer PyrisDiamond TG-DTA instrument under an N_2 atmosphere using a heating rate of 5 °C min^{-1} from room temperature up to 1000 °C. Magnetic properties were performed on a Superconducting Quantum Interference Device (SQUID) magnetometer. The diamagnetism of all constituent atoms was corrected with Pascal's constant.

Single crystal X-ray crystallography.

Diffraction data for the complex were collected on a ROD, Synergy Custom DW system, HyPix diffractometer (Mo-Kα radiation and λ = 0.71073 Å) in Φ and ω scan modes. The structures were solved by direct methods, and refined by a full-matrix least-squares method on the basis of F^2 by using SHELXL. Anisotropic thermal parameters were applied to all non-hydrogen atoms. Hydrogen atoms were generated geometrically. The crystallographic data for clusters **1** are listed in Table S1, and selected bond lengths and angles are given in Table S2. The CCDC reference number for the crystal structures of cluster **1** is 2260488.

HRESI-MS measurement.

HRESI-MS measurements were conducted at a capillary temperature of 275 °C. Aliquots of the solution were injected into the device at 2 μL. The mass spectrometer used for the measurements was a ThermoExactive and the data were collected in positive and negative ion modes. Thespectrometer was previously calibrated with the standard tune mix to give a precision of *ca*. 2 ppm. within the region of m/z = 200−4000. The capillary voltage was 50 V, the tube lens voltage was 150 V, and the skimmer voltage was 25 V.

[1] Sheldrick, G. M. *Acta Crystallogr., Sect. C: Struct. Chem*. **2015**, *71*, 3-8.

The synthesis method.

Synthesis of 1: A mixture of 2-pyridinecarbohydrazide (0.2 mmol, 27.4 mg), 2,3,4-trihydroxybenzaldehyde (0.2 mmol, 30.8 mg) and mixed metal salt ($Dy(NO_3)_3·6H_2O$:$DyCl_3·6H_2O$ = 1:1) and triethylamine (60 μL) were dissolved in mixed solvent (CH_3OH:CH_3CN = 1:1) in a Pyrex tube. The tube was sealed and heated at 80 °C in an oven for 2 days, brown-red crystals were observed with a yield of about 46% (based on $Dy(NO_3)_3·6H_2O$). Elemental analysis theoretical value ($C_{116}H_{116}Cl_2Dy_9N_{24}O_{48}$): C, 33.56%; H, 2.79%; N,8.10%; experimental value: C, 33.52%; H, 2.71%; N, 8.06%. Infrared spectrum data (IR, KBr pellet, cm^{-1}): 3855 (m), 3750 (s), 3404 (m), 1612 (m), 1574 (m), 1441 (m), 1383 (w), 1269 (w), 1069 (m), 1029 (s), 737 (m), 628 (m), 543 (m).

Table S1. Crystallographic data of the cluster **1**.

	1
Empirical formula	$C_{116}H_{116}Cl_2Dy_9N_{24}O_{48}$
Formula weight	4147.72
T, K	293(2)
Crystal system	tetragonal
Space group	$P4/n$
a, Å	25.0121(4)
b, Å	25.0121(4)
c, Å	14.3000(7)
α, °	90
β, °	90
γ, °	90
V, Å^3	8946.2(5)
Z	2
D_c, g cm^3	1.575
μ, mm^{-1}	3.809
$F(000)$	3984.0
2θ range for data collection/°	4.606 to 50.05
Reflns coll.	33549
Unique reflns	7896
R_{int}	0.0456
R_1[a] ($I > 2\sigma(I)$)	0.0649
wR_2[b] (all data)	0.1855
GOF	1.051

[a]$R_1 = \Sigma||F_o|-|F_c||/\Sigma|F_o|$, [b]$wR_2 = [\Sigma w(F_o^2-F_c^2)^2/\Sigma w(F_o^2)^2]^{1/2}$

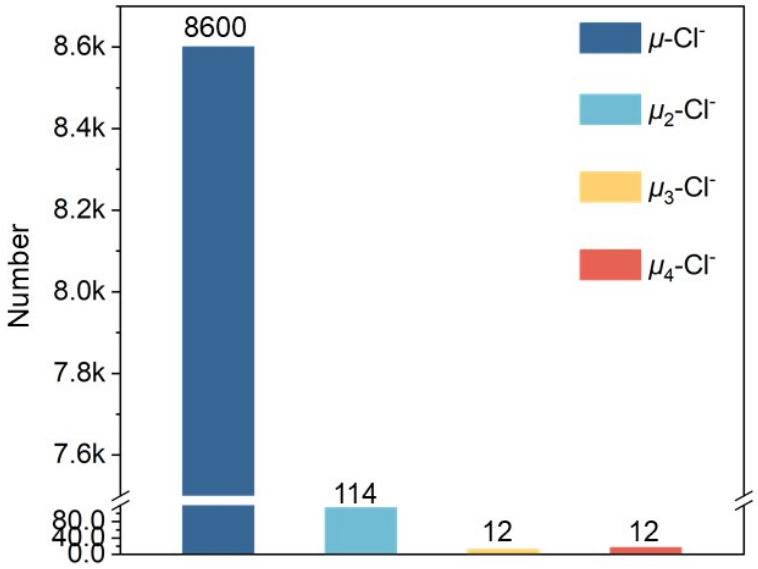

Figure S1. Using CCDC's literature survey results for μ-Cl$^-$, μ_2-Cl$^-$, μ_3-Cl$^-$, and μ_4-Cl$^-$.

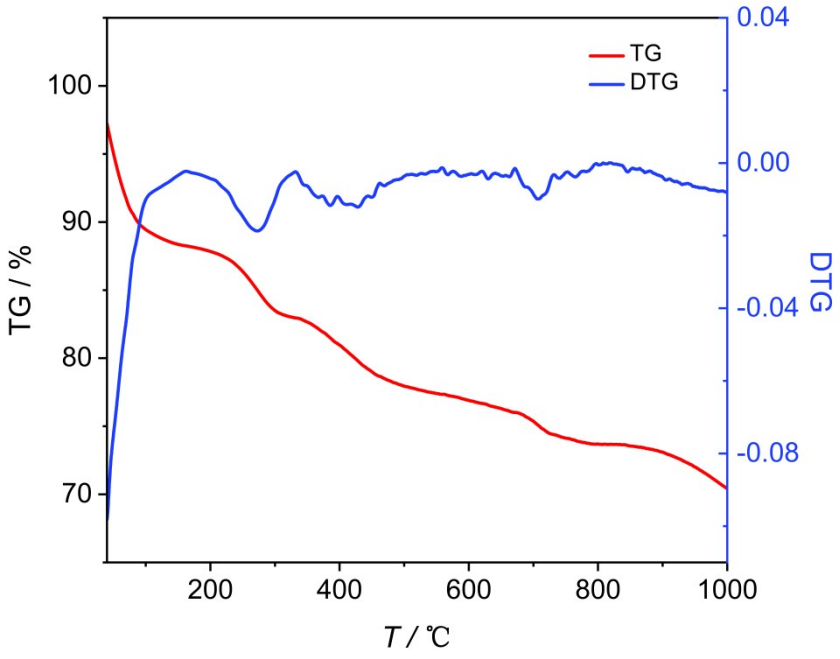

Figure S2. TG-DTG curves of cluster **1**.

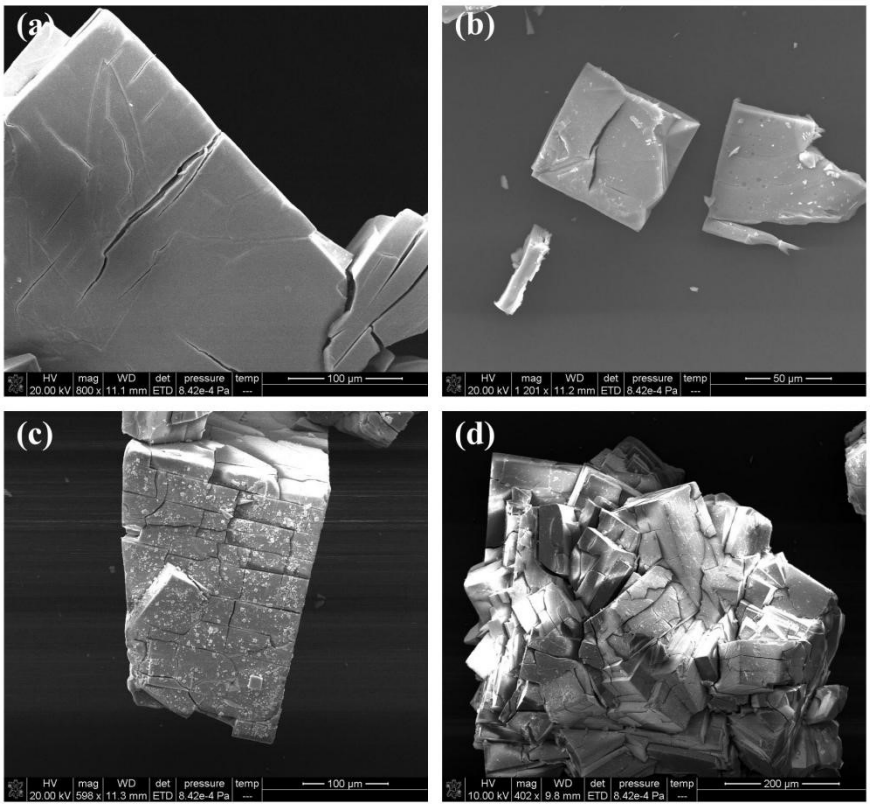

Figure S3. SEM image of cluster **1** (a-b) and after 720 min (c-d).

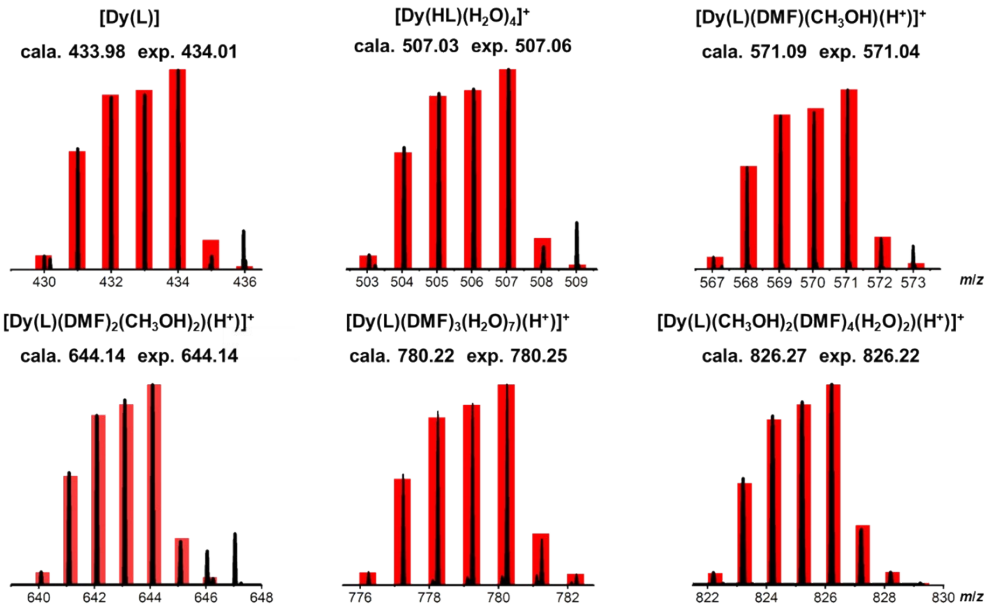

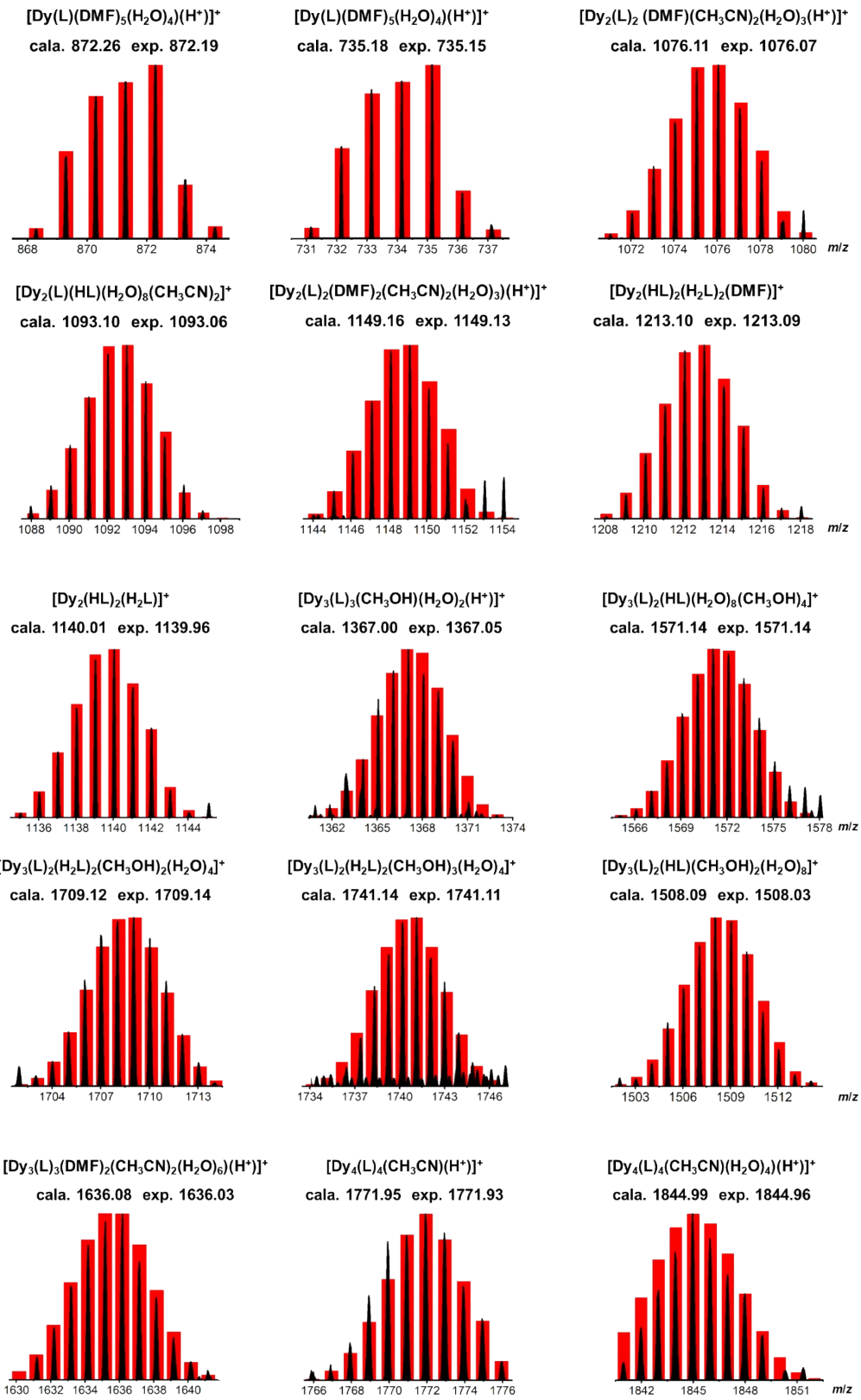

Figure S4. Time-dependent HRESI-MS spectra for the assembly of cluster **1** in positive mode.

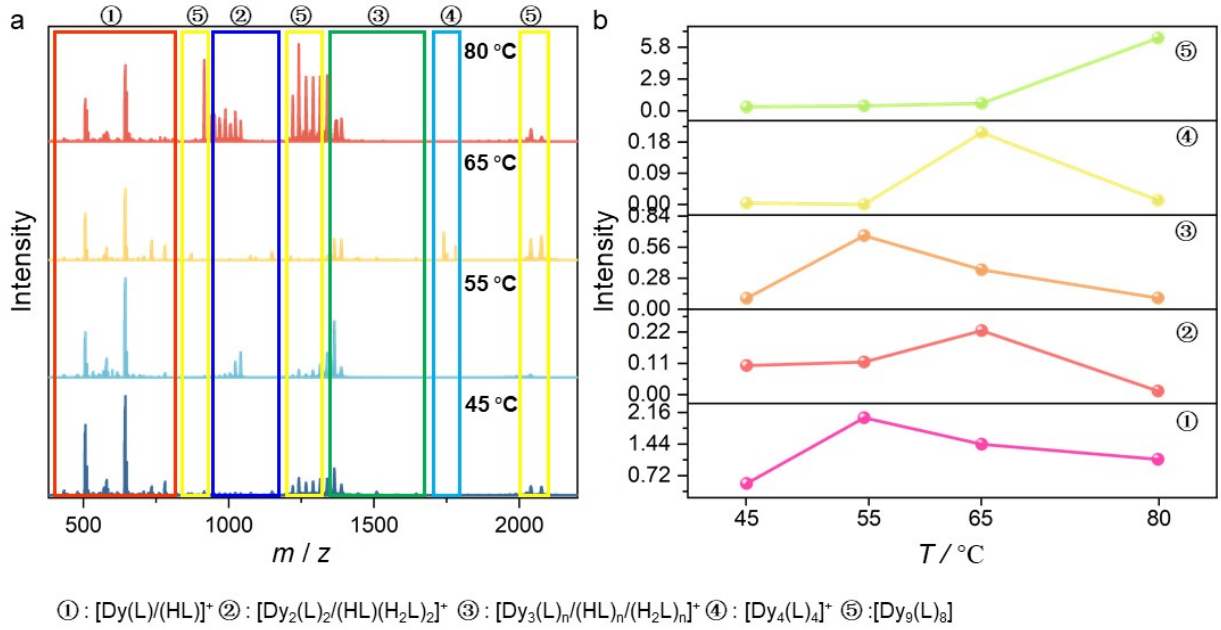

Figure S5. HRESI-MS spectrum of cluster **1** at different temperatures (a), the intensity of each fragment varies with temperature (b).

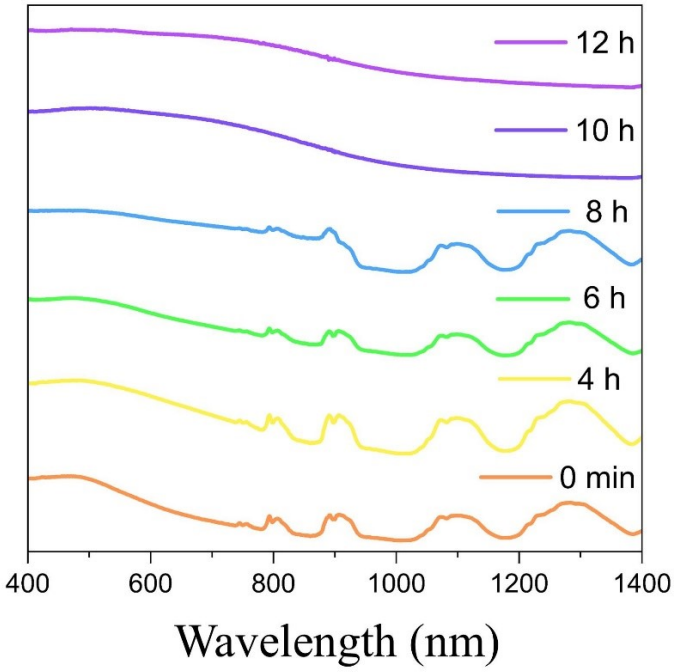

Figure S6. UV-Vis spectrograms of cluster **1** after exposing to air at different times.

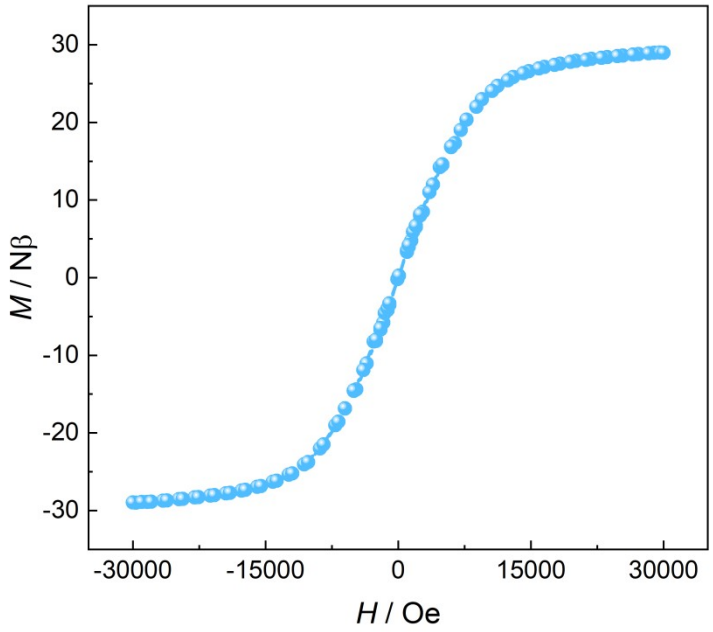

Figure S7. Loop curve graph of cluster **1** at 2 K.

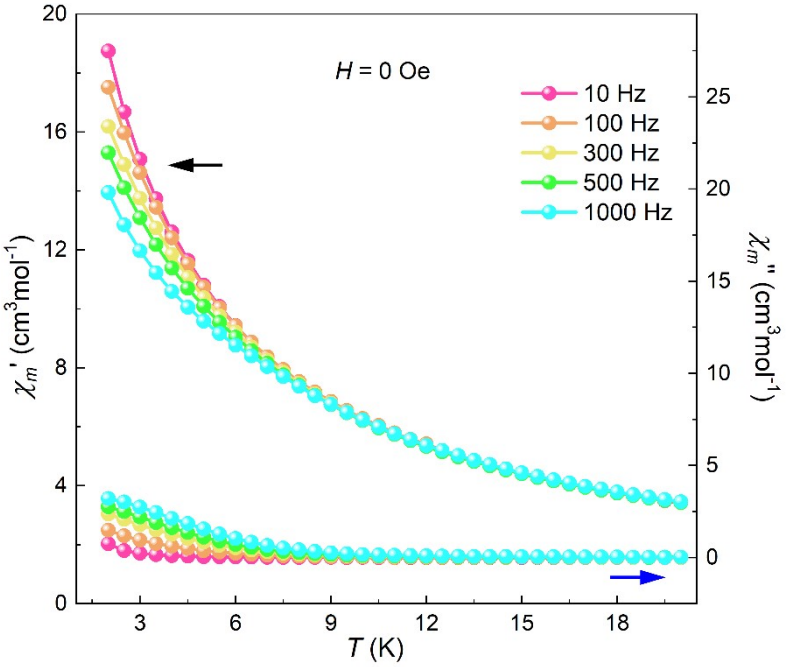

Figure S8. Temperature dependence of the real (χ') and imaginary (χ'') ac susceptibilities at different frequencies in the 0 Oe dc fields for cluster **1**.

Table S2. Selected bond lengths (Å) and angles (°) of cluster **1**.

Bond lengths (Å)					
Dy1-O4	2.288(8)	Dy2^{iii}-O1	2.363(8)	Dy4^{iii}-O1	2.520(13)
Dy1-O1^{ii}	2.334(9)	Dy2^{i}-Cl1	2.901(3)	Dy4-N6	2.625(11)
Dy1-O9	2.351(9)	Dy2^{iii}-Cl1	2.901(3)	Dy4-O1^{ii}	2.520(13)
Dy1-O10	2.380(8)	Dy2^{ii}-Cl1	2.901(3)	Dy4-O5	2.214(16)
Dy1-O6	2.393(10)	Dy2^{iii}-O2	2.248(9)	Dy5-Cl1	2.894(6)
Dy1-O7	2.413(8)	Dy3-O11	2.373(7)	Dy5^{i}-Cl1	2.894(6)
Dy1-O5	2.501(10)	Dy3-O11^{i}	2.373(7)	Dy5^{iii}-Cl1	2.894(6)
Dy1-N1	2.578(11)	Dy3-O11^{ii}	2.373(7)	Dy5^{ii}-Cl1	2.894(6)
Dy1-N6	2.605(10)	Dy3-O11^{iii}	2.373(7)	Dy5-O11	2.364(10)
Dy1^{iii}-O1	2.334(8)	Dy3-O13^{i}	2.507(9)	Dy5-O2	2.183(12)
Dy2-O2^{ii}	2.249(9)	Dy3-O13^{iii}	2.507(9)	Dy5^{iii}-O2	2.440(12)
Dy2-O10	2.313(8)	Dy3-O13^{ii}	2.507(9)	Dy5-O3	2.519(11)
Dy2-O4	2.318(9)	Dy3-O13	2.507(9)	Dy5^{iii}-O1	2.474(11)
Dy2-O11	2.335(8)	Dy3-Cl1	2.934(5)	Dy5-O4	2.202(11)
Dy2-O1^{ii}	2.363(8)	Dy4-O7	2.400(9)	Dy5-O2^{ii}	2.440(12)
Dy2-O2	2.386(8)	Dy4-O6	2.538(13)	Dy5-O1^{ii}	2.474(11)
Dy2-O3	2.554(9)	Dy4-O9	2.652(16)		
Dy2-Cl1	2.901(3)	Dy4-O4	2.121(11)		
Bond angles (°)					
O4-Dy1-O1^{ii}	68.0(3)	O4-Dy2-O1^{ii}	67.1(3)	O4-Dy4-O5	82.9(6)
O4-Dy1-O9	142.8(3)	O11-Dy2-O1^{ii}	130.8(3)	O4-Dy4-N1	73.6(4)
O1^{ii}-Dy1-O9	76.2(3)	O2^{ii}-Dy2-O2	144.0(3)	O5-Dy4-N1	78.1(6)
O4-Dy1-O10	70.3(3)	O10-Dy2-O2	108.4(3)	O4-Dy4-O7	149.9(7)
O1^{ii}-Dy1-O10	69.0(3)	O4-Dy2-O2	68.8(3)	O5-Dy4-O7	76.9(4)
O9-Dy1-O10	87.9(3)	O11-Dy2-O2	86.6(3)	N1-Dy4-O7	80.5(4)
O4-Dy1-O6	112.4(3)	O1^{ii}-Dy2-O2	133.6(3)	O4-Dy4-O1^{ii}	67.1(4)
O1^{ii}-Dy1-O6	83.2(3)	O2^{ii}-Dy2-O3	81.6(3)	O5-Dy4-O1^{ii}	146.9(5)
O9-Dy1-O6	71.9(3)	O10-Dy2-O3	144.6(3)	N1-Dy4-O1^{ii}	104.9(4)
O10-Dy1-O6	149.0(3)	O4-Dy2-O3	80.5(3)	O7-Dy4-O1^{ii}	136.1(6)
O4-Dy1-O7	136.5(3)	O11-Dy2-O3	144.2(3)	O4-Dy4-O6	113.0(4)
O1^{ii}-Dy1-O7	148.1(3)	O1^{ii}-Dy2-O3	80.4(3)	O5-Dy4-O6	130.3(5)
O9-Dy1-O7	80.5(3)	O2-Dy2-O3	79.0(3)	N1-Dy4-O6	63.8(4)

O10-Dy1-O7	131.9(3)	O10-Dy2-O1^{ii}	69.7(3)	O7-Dy4-O6	66.8(4)
O6-Dy1-O7	68.9(3)	O11^{ii}-Dy3-Cl1	68.95(18)	O1^{ii}-Dy4-O6	76.7(4)
O4-Dy1-O5	73.5(3)	O11^{iii}-Dy3-Cl1	68.95(18)	O4-Dy4-N6	128.7(5)
O1^{ii}-Dy1-O5	139.7(3)	O13^{i}-Dy3-Cl1	131.4(2)	O5-Dy4-N6	70.4(4)
O9-Dy1-O5	137.0(3)	O13^{iii}-Dy3-Cl1	131.4(2)	N1-Dy4-N6	136.7(5)
O10-Dy1-O5	87.3(3)	O13^{ii}-Dy3-Cl1	131.4(2)	O7-Dy4-N6	64.3(3)
O6-Dy1-O5	123.6(4)	O13-Dy3-Cl1	131.4(2)	O1^{ii}-Dy4-N6	117.8(5)
O7-Dy1-O5	71.5(3)	O11^{i}-Dy3-O13	151.1(3)	O6-Dy4-N6	117.8(5)
O4-Dy1-N1	67.5(3)	O11^{ii}-Dy3-O13	121.7(3)	O4-Dy4-O9	133.9(5)
O1^{ii}-Dy1-N1	104.9(3)	O11^{iii}-Dy3-O13	87.1(3)	O5-Dy4-O9	136.1(4)
O9-Dy1-N1	134.3(4)	O13^{i}-Dy3-O13	97.2(4)	N1-Dy4-O9	128.3(5)
O10-Dy1-N1	136.1(3)	O13^{iii}-Dy3-O13	64.1(2)	O7-Dy4-O9	74.9(4)
O6-Dy1-N1	63.2(4)	O13^{ii}-Dy3-O13	64.1(2)	O1^{ii}-Dy4-O9	67.9(4)
O7-Dy1-N1	76.6(3)	O11-Dy3-Cl1	68.95(18)	O6-Dy4-O9	64.9(4)
O5-Dy1-N1	69.8(4)	O11^{i}-Dy3-Cl1	68.95(18)	N6-Dy4-O9	67.2(4)
O4-Dy1-N6	122.1(3)	O11-Dy3-O13^{ii}	87.1(3)	O2-Dy5-O4	74.7(4)
O1^{ii}-Dy1-N6	126.2(3)	O11^{i}-Dy3-O13^{ii}	121.7(3)	O2-Dy5-O11	90.7(4)
O9-Dy1-N6	72.0(3)	O11^{ii}-Dy3-O13^{ii}	66.4(3)	O4-Dy5-O11	128.5(4)
O10-Dy1-N6	67.5(3)	O11^{iii}-Dy3-O13^{ii}	151.1(3)	O2-Dy5-O2^{ii}	144.8(4)
O6-Dy1-N6	124.3(3)	O13^{i}-Dy3-O13^{ii}	64.1(2)	O4-Dy5-O2^{ii}	132.2(4)
O7-Dy1-N6	64.4(3)	O13^{iii}-Dy3-O13^{ii}	97.2(4)	O11-Dy5-O2^{ii}	86.6(4)
O5-Dy1-N6	66.7(3)	O11-Dy3-O13	66.4(3)	O2-Dy5-O1^{ii}	139.1(4)
N1-Dy1-N6	128.4(4)	O13^{i}-Dy3-O13^{iii}	64.1(2)	O4-Dy5-O1^{ii}	66.9(4)
O1^{ii}-Dy2-Cl1	139.2(2)	O11-Dy3-O11^{i}	137.9(4)	O11-Dy5-O1^{ii}	123.9(4)
O2-Dy2-Cl1	72.0(2)	O11-Dy3-O11^{ii}	82.59(12)	O2^{ii}-Dy5-O1^{ii}	66.3(3)
O3-Dy2-Cl1	74.4(2)	O11^{i}-Dy3-O11^{ii}	82.59(12)	O2-Dy5-O3	83.6(4)
O4-Dy2-Cl1	136.6(2)	O11-Dy3-O11^{iii}	82.59(12)	O4-Dy5-O3	83.5(4)
O11-Dy2-Cl1	70.0(2)	O11^{i}-Dy3-O11^{iii}	82.59(12)	O11-Dy5-O3	144.7(4)
O2^{ii}-Dy2-Cl1	73.7(2)	O11^{ii}-Dy3-O11^{iii}	137.9(4)	O2^{ii}-Dy5-O3	78.8(3)
O10-Dy2-Cl1	141.0(2)	O11-Dy3-O13^{i}	151.1(3)	O1^{ii}-Dy5-O3	79.0(3)
O2^{ii}-Dy2-O10	105.0(3)	O11^{i}-Dy3-O13^{i}	66.4(3)	O2-Dy5-Cl1	74.8(3)
O2^{ii}-Dy2-O4	136.7(3)	O11^{ii}-Dy3-O13^{i}	87.1(3)	O4-Dy5-Cl1	144.3(4)
O10-Dy2-O4	71.0(3)	O11^{iii}-Dy3-O13^{i}	121.7(3)	O11-Dy5-Cl1	69.8(3)

O2^{ii}-Dy2-O11	91.9(3)	O11-Dy3-O13^{iii}	121.7(3)	O2^{ii}-Dy5-Cl1	71.4(2)
O10-Dy2-O11	71.0(3)	O11^{i}-Dy3-O13^{iii}	87.1(3)	O1^{ii}-Dy5-Cl1	133.6(4)
O4-Dy2-O11	124.2(3)	O11^{ii}-Dy3-O13^{iii}	151.1(3)	O3-Dy5-Cl1	75.1(3)
O2^{ii}-Dy2-O1^{ii}	71.2(3)	O11^{iii}-Dy3-O13^{iii}	66.4(3)		

Table S3. *SHAPE* analysis of the Dy(III) in cluster **1**.

Label	**Shape**	**Symmetry**	**Distortion** (°) **Dy1**
EP-9	D_{9h}	Enneagon	35.359
OPY-9	C_{8v}	Octagonal pyramid	25.136
HBPY-9	D_{7h}	Heptagonal bipyramid	17.247
JTC-9	C_{3v}	Triangular cupola J3	16.363
JCCU-9	C_{4v}	Capped cube (J8)	3.528
CCU-9	C_4	Capped cube	3.245
JCSAPR-9	C_{4v}	Capped sq. antiprism	2.595
CSAPR-9	C_{4v}	Capped square antiprism	2.612
JTCTPR-9	D_{3h}	Tricapped trigonal prism J51	4.254
TCTPR-9	D_{3h}	Tricapped trigonal prism	3.918
JTDIC-9	C_{3v}	Tridiminished icosahedron J63	13.641
HH-9	C_{2v}	Hula-hoop	9.209
MFF-9	C_s	Muffin	3.309
Label	**Shape**	**Symmetry**	**Distortion** (°) **Dy2**
OP-8	D_{8h}	Octagon	44.543
HPY-8	C_{7v}	Heptagonal pyramid	34.731
HBPY-8	D_{6h}	Hexagonal bipyramid	31.851
CU-8	O_h	Cube	33.204
SAPR-8	D_{4d}	Square antiprism	26.712
TDD-8	D_{2d}	Triangular dodecahedron	25.028
JGBF-8	D_{2d}	Johnson-Gyrobifastigium (J26)	30.173
JETBPY-8	D_{3h}	Johnson-Elongated triangular bipyramid (J14)	39.148
JBTP-8	C_{2v}	Johnson-Biaugmented trigonal prism (J50)	23.235
BTPR-8	C_{2v}	Biaugmen tedtrigonal prism	24.692
JSD-8	D_{2d}	Snub disphenoid (J84)	23.435
TT-8	T_d	Triakis tetrahedron	31.640
ETBPY-8	D_{3h}	Elongated trigonal bipyramid	39.560
Label	**Shape**	**Symmetry**	**Distortion** (°) **Dy3**
EP-9	D_{9h}	Enneagon	43.947
OPY-9	C_{8v}	Octagonal pyramid	34.007
HBPY-9	D_{7h}	Heptagonal bipyramid	33.529
JTC-9	C_{3v}	Triangular cupola J3	23.678

JCCU-9	C_{4v}	Capped cube (J8)	27.364
CCU-9	C_4	Capped cube	26.975
JCSAPR-9	C_{4v}	Capped sq. antiprism	20.866
CSAPR-9	C_{4v}	Capped square antiprism	20.952
JTCTPR-9	D_{3h}	Tricapped trigonal prism J51	20.560
TCTPR-9	D_{3h}	Tricapped trigonal prism	21.287
JTDIC-9	C_{3v}	Tridiminished icosahedron J63	29.525
HH-9	C_{2v}	Hula-hoop	27.757
MFF-9	C_s	Muffin	21.479

Table S4. Major species assigned in the Time-dependent HRESI-MS of cluster **1** in positive mode.

Peaks	***Exp. m/z***	***Calc. m/z***
[Dy(L)]	434.01	433.98
$[Dy(HL)(H_2O)_4]^+$	507.06	507.03
$[Dy(L)(DMF)(CH_3OH)(H^+)]^+$	571.04	571.09
$[Dy(L)(DMF)_2(CH_3OH)_2(H^+)]^+$	644.14	644.14
$[Dy(L)(DMF)_3(H_2O)_7(H^+)]^+$	780.25	780.22
$[Dy(L)(CH_3OH)_2(DMF)_4(H_2O)_2(H^+)]^+$	826.22	826.27
$[Dy(L)(DMF)_5(H_2O)_4(H^+)]^+$	872.19	872.26
$[Dy(L)(DMF)_5(H_2O)_4(H^+)]^+$	735.15	735.18
$[Dy_2(L)_2(DMF)(CH_3CN)_2(H_2O)_3(H^+)]^+$	1076.07	1076.11
$[Dy_2(L)(HL)(H_2O)_8(CH_3CN)_2]^+$	1093.06	1093.10
$[Dy_2(L)_2(DMF)_2(CH_3CN)_2(H_2O)_3(H^+)]^+$	1149.13	1149.16
$[Dy_2(HL)_2(H_2L)_2(DMF)]^+$	1213.09	1213.10
$[Dy_2(HL)_2(H_2L)]^+$	1139.96	1140.01
$[Dy_3(L)_3(CH_3OH)(H_2O)_2(H^+)]^+$	1367.05	1367.00
$[Dy_3(L)_2(HL)(H_2O)_8(CH_3OH)_4]^+$	1571.14	1571.14
$[Dy_3(L)_2(H_2L)_2(CH_3OH)_2(H_2O)_4]^+$	1709.14	1709.12
$[Dy_3(L)_2(H_2L)_2(CH_3OH)_3(H_2O)_4]^+$	1741.11	1741.14
$[Dy_3(L)_2(HL)(CH_3OH)_2(H_2O)_8]^+$	1508.03	1508.09
$[Dy_3(L)_3(DMF)_3(CH_3CN)_2(H_2O)_2(H^+)]^+$	1636.03	1636.08
$[Dy_4(L)_4(CH_3CN)(H^+)]^+$	1771.93	1771.95
$[Dy_4(L)_4(CH_3CN)(H_2O)_4(H^+)]^+$	1844.96	1844.99
$[Dy_9(L)_8Cl(CH_3OH)_8(H_2O)_2(H^+)_3]^{5+}$	790.99	790.99
$[Dy_9(L)_8Cl(CH_3OH)_8(H_2O)_6(H^+)_3]^{5+}$	805.61	805.61
$[Dy_9(L)_8(CH_3OH)_8(H_2O)_4(DMF)_2(H_2O)_2(H^+)_2]^{5+}$	835.20	835.24
$[Dy_9(L)_8Cl(CH_3OH)_8(H_2O)_2(H^+)_2]^{4+}$	988.49	988.49
$[Dy_9(L)_8Cl(CH_3OH)_8(H_2O)_4(DMF)(H^+)_2]^{4+}$	1015.99	1016.01
$[Dy_9(L)_8Cl(CH_3OH)_9(H_2O)(CH_3CN)_3(H^+)_2]^{4+}$	1022.77	1022.76
$[Dy_9(L)_8Cl(CH_3OH)_8(H_2O)_5(DMF)(CH_3CN)_2(H^+)]^{4+}$	1040.77	1040.78
$[Dy_9(L)_8(CH_3OH)_7(H_2O)]^{3+}$	1289.95	1289.99